Ground state dynamically stable phases for fluorine in the TPa pressure regime by evolutionary algorithms

B. H. Cogollo-Olivo and J. A. Montoya

Universidad de Cartagena, Instituto de Matemáticas Aplicadas, 130001, Cartagena de Indias, Colombia.

Received 30 November 2022; accepted 22 March 2023

In this work, we tested *ab initio* methods combined with evolutionary algorithms for searching stable crystalline structures for solid fluorine in the Tera-Pascal (TPa) regime. We performed several structural searches using the USPEX code, at pressures that spanned the range from 1 to 5 TPa, considering up to 16 atoms per unit-cell for selected pressures. Our findings partially support recent studies by validating the transformation of fluorine from a molecular form, $Cmca$, into an intermediate polymeric form before its eventual dissociation. Enthalpy comparisons between candidate structures of fluorine at high pressure show a direct transition from the molecular phase $Cmca$ into a $Pm\bar{3}n$ extended structure at 2.7 TPa, the later consisting of linear chains and independent atoms, which disagrees with previous conflicting reports that proposed two other intermediate phases to also exist as stable crystalline forms close to 3 TPa at zero temperature.

Keywords: Density functional calculations; fluorine; structural prediction; enthalpy; molecular solids

DOI: https://doi.org/10.31349/RevMexFis.69.041606

1. Introduction

Under extreme conditions of pressure and temperature, the chemistry of materials, as we know it, changes drastically, making it possible to access new states of matter. Thus, experimental and theoretical research under extreme conditions have been fundamental in their contribution to geophysics, planetary sciences, and mineralogy, as well as to the characterization of new materials of technological interest and their respective phase diagrams, leading to a better understanding of their physical and chemical properties. In this sense, the fundamental study of diatomic molecules of single elements with low atomic numbers subjected to high-pressure conditions, has been the subject of great interest by the scientific community due to the theoretical and experimental detection of phenomena, such as the eventual metallization induced by pressure or phase transformations observed in analogous mono-atomic systems such as nitrogen [1, 2] and the halogen elements [3–6]. Fluorine is the first of the halogens and the last of the diatomic elements of the first row in the periodic table. It was chosen as the study object of this work given its similarities with hydrogen and the high energy density of its electronic bonds, likewise, it is an abundant element in the universe and is particularly interesting for its high oxidizing capacity and for having the highest electronegativity among all elements, followed by oxygen's.

Despite the above reasons, fluorine has not been studied very extensively if compared to other single-element diatomic molecules (H_2, N_2, O_2, Cl_2, Br_2, and I_2). For instance, the space group of solid fluorine at high pressure remained controversial for many years because two different structures were proposed through spectroscopy studies and theoretical calculations, respectively [7–10]. Experiments were carried out using diamond anvil cells (DAC), but it was very challenging to obtain reliable results [10,11]. In addition to the very small sample sizes that are typical of experiments involving DACs, other technical difficulties came from the fact that fluorine and other halogen elements are characterized by being volatile, corrosive, and highly reactive, increasing the complexity level when studied in the lab. For this reason, it was not until a few years ago that, by using computational techniques, a study established that the $C2/c$ structure is energetically more stable than $C2/m$, which then transforms into $Cmca$ at 8 Giga-Pascals (GPa) [12] and not reporting any other structural transformation up to the pressure-limit of that work, which was 100 GPa. In their study, Olson *et al.* [13] spanned a higher pressure range covering up to a few Tera-Pascals (TPa); not only they corrected the transition from $C2/c$ to $Cmca$ by placing it at 70 GPa, but also reported a phase transition to $P4_2/mmc$ and then to $Pm\bar{3}n$, at 2.5 and 3.0 TPa, respectively. Additionally, the study by Olson *et al.* [13] included a structural search component: their work made use of a methodology that has undergone recently a process of refinement called Symmetry Driven Structure Search (SYDSS) [14]; this method is based on sampling space groups and Wyckoff positions to propose new crystal structures. In Ref. [13], the structural search for high-pressure phases received as starting point a set of structures previously reported for lower pressures and some restrictions were imposed to generate new systems, *i.e.*, the bond lengths and the number of atoms in the molecules. More recently, Duan *et al.* [15] presented enthalpy relations for some predicted phases of fluorine up to 30 TPa based on the *ab initio* random structure searching (AIRSS) method [16]. In the structural sequence reported in that work, fluorine undergoes two intermediate transitions, namely $P6/mmc$ and $Pm\bar{3}n$, at 2.7 and 4.0 TPa, respectively, before dissociating into the $Fddd$ atomic phase at 30 TPa.

Given the substantial differences observed in recent theoretical reports at TPa pressures for solid fluorine, validating the structures found in Refs. [13, 15] is necessary. For this study, we chose the computational tool for crystal structure determination known as USPEX [17–20], which is currently one of the most reliable codes used within the materials science community and combines *ab-initio* methods with structure prediction techniques based on evolutionary algorithms. In the past, USPEX has been able to predict new phases of materials at high pressure, including some up to 350 GPa that are relevant to the Earth's interior, allowing new ways of understanding matter at extreme conditions.

In this work, we tested USPEX's abilities by performing meticulous structural searches of fluorine crystalline phases, varying the number of atoms per unit cell and repeating this process at different volumes that correspond to TPa conditions of pressure. All this, interfaced with Quantum ESPRESSO [21,22] as the selected tool for accurate *ab-initio* structural relaxations, as detailed in the Methods section. The Results and Discussion section provides our research's findings and analysis for several candidate-structures. Finally, we present our main conclusions in the last section, by providing answers regarding the coordination nature, electronic character and range of stability of fluorine's high pressure phases in the range from 1 to 5 TPa.

TABLE I. Structural information of previously reported structures for high-pressure phases of fluorine.

Space group Pressure	Lattice parameters (Å,°)	Atomic coordinates (fractional)
(64) $Cmca$	$a = 4.31$	$8f$
0.02 TPa	$b = 2.88$	$y = 0.3799$
Ref. [12]	$c = 5.84$	$z = 1.3933$
	$\alpha = \beta = \gamma = 90$	
(131) $P4_2/mmc$	$a = 2.69$	$2a$
2.75 TPa	$b = c = 2.60$	$2d$
Ref. [13]	$\alpha = \beta = \gamma = 90$	
(192) P_6/mcc	$a = 3.68$	$2a$
3.00 TPa	$b = c = 2.65$	$12l$
Ref. [15]	$\alpha = \beta = 90$	$x = 0.1097$
	$\gamma = 120$	$y = 0.6831$
(223) $Pm\bar{3}n$	$a = 2.59$	$2a$
3.15 TPa	$\alpha = \beta = \gamma = 90$	$6d$
Ref. [13]		
5.00 TPa	$a = 2.44$	$2a$
Ref. [15]	$\alpha = \beta = \gamma = 90$	$6c$

2. Methods

In view of the previous contradicting results, regarding the predicted sequence of transitions when going from molecular to extended forms of solid fluorine, the main objective of this work is to provide an independent insight by using a different methodological approach for performing the structural search of novel phases of this element in the Tera-Pascal regime. Over the past years, the likelihood of obtaining reliable results with computing methods for crystal structure prediction has been improved substantially. In this work, we have selected the USPEX package for its proven robustness in pressure regimes similar to the one of this study. In the initial stage we used USPEX to successfully generate good candidate structures for solid fluorine, followed by density functional theory (DFT) calculations for the structural optimization and refinement of selected candidate phases at different pressures. In addition, the density functional perturbation theory (DFPT) scheme allowed us to determine the dynamical stability of the structures that were found, from vibrational data.

2.1. USPEX calculations

USPEX employs an evolutionary algorithm to generate different structures of solid crystals, which is mostly unbiased because it only uses information that the researcher provides about the number and type of atoms to be contained within the crystalline unit cell [17–20]. At first, the initial set of structures is generated by randomly choosing any crystal space group. Thus, this first generation is mainly composed of arbitrary far-of-equilibrium structures. It is then necessary to perform a structural relaxation to decrease and determine the total internal energy of each candidate system and use that value as a fitness criterion. Then, after a purely random start, new generations are created via genetic operations which can apply criteria such as heredity, mutation, and permutation; nevertheless, a portion of the new structures is still made randomly to ensure a level of diversity in each generation. The structural search ends when one of these criteria is achieved: no new *best structure* is generated for a certain number of generations, or, the set value for the maximum number of generations is reached.

Here, fixed composition searches were conducted to determine suitable high-pressure phases for solid fluorine. USPEX-based structure predictions were performed independently on different cell sizes, containing 2, 4, 6, 8, 12, and 16 atoms, in a pressure range spanning from 1.0 to 5.0 TPa in steps of 0.5 TPa, with the exception of 1.5 TPa that was not considered explicitly in this work but interpolated instead. Also, the two biggest cell sizes (12 and 16 atoms) were studied at four selected pressures instead of eight, and interpolated for the other pressures in that same range. The USPEX calculations started with an initial population of 30 structures, generated randomly with no restrictions on the space groups that could be assigned to the structures. In addition, no seeds or anti-seeds were considered. Subsequent generations were produced by applying the following variation operations (in parenthesis are the weights used in this work):

heredity (50%), soft-mutation (15%), lattice mutation (10%), and permutation (5%), while the rest of the newly generated structures (20%) were still randomly produced with the random symmetric structure generator to assure diversity as explained earlier. We set the maximum number of generations to 50, and the convergence criterion was set to 20 repetitions of the same prediction. All USPEX calculations ended by reaching the *repeated best structure* convergence criterion.

2.2. DFT Calculations

The trial structures were optimized in a low-to-high precision process using first-principles DFT calculations using the Quantum Espresso suite [21, 22] for variable-cell relaxation. We increased the convergence criteria and precision settings at each step, with a reciprocal space resolution for k-point generation of 0.20, 0.16, and 0.12 2π/Å, respectively. The k-point grids for the Brillouin zone integration were generated with the Monkhorst-Pack method [23]. Finally, all DFT calculations were performed using the plane-wave pseudopotential method with projector-augmented wave (PAW) pseudopotentials [24]. For the calculation of the exchange and correlation functionals, generalized gradient approximation (GGA) combined with Perdew-Burke-Ernzerhof (PBE) [25] parametrization was used. With the calculated lattice enthalpy after total relaxation, the structures were sorted from the lowest to the highest to be later used as input for the next generation.

3. Results and discussion

We began our exploration by first keeping present the structures that were reported in previous studies up to 5.0 TPa [12, 13, 15]: $Cmca$, $P4_2/mmc$, $P6/mcc$, $Pm\bar{3}n$. Their structural parameters are detailed in Table I for future reference and comparisons.

3.1. Structural search process

In total, nearly 30000 fluorine structures with 2-16 atoms per unit cell spanning the pressure range of 1 to 5 TPa were generated in 40 different runs, via USPEX combined with DFT, using the Quantum ESPRESSO suite. As explained earlier, the first generation of each run consists of randomly generated structures. After that, the act of creating a new candidate structure usually follows a two-step procedure. First, the evolutionary algorithm enables the generation of a new system using one of three operations [17–20]:

- *Heredity* combines two or more parent structures to create a new one, allowing a broad search of the energy landscape while preserving fragments of good structures.
- *Permutation* randomly swaps chosen pairs of atoms within the unit cell, which facilitates finding the optimal ordering of the atoms.

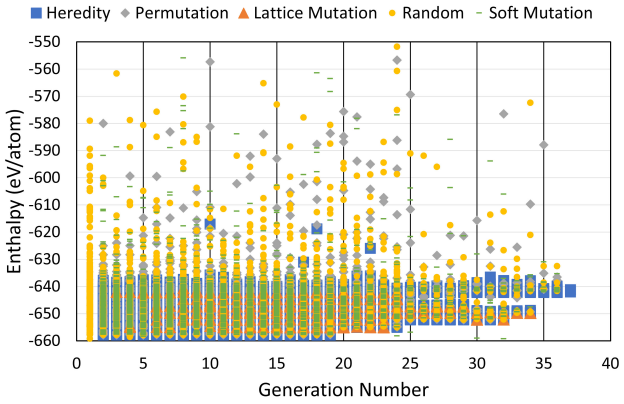

FIGURE 1. Enthalpy distribution, in eV per atom, of structures generated during 40 different runs for fluorine with 2-16 atoms per unit cell and at 1-5 TPa. The symbols represent the origin of generated structures: random generation (yellow circles) or as a result of certain genetic operations: heredity (blue squares), permutation (grey rhombus), lattice mutation (orange triangles), and soft mutation (green dash).

- *Mutation* creates a child structure from a single parent, retaining some characteristics from it while introducing new structural features. There are two main types of mutations: *lattice mutation*, that randomly distorts the cell shape, allowing a better exploration of the neighborhood of parent structures and preventing premature convergence of the lattice; and *soft-mutation*, which moves the atoms along the eigenvectors of the softest modes in order to create a new structure across the lowest energy barrier, allowing a local and semi-local exploration of the energy landscape.

Each run contemplates the use of the genetic operations described above, together with a percentage of randomly generated structures. Figure 1 shows the enthalpy distribution of the generated systems within all 40 runs performed. We can see that randomly generated structures (yellow circles) with those from permutation operations (grey rhombus) and up to some extent also the ones from soft mutation (green dashes) span a large energy interval. In contrast, most relevant structures are created due to heredity (blue squares) and lattice mutation (orange triangles).

3.2. Crystal structure determination

From USPEX predictions, 14 different crystal structures emerged as potential candidates for fluorine in the terapascal regime. These structures included all those previously reported that were compatible with our cell sizes (*i.e.*, except for $P6/mcc$ which contains 14 atoms per cell, since this size was not included in our study) and also a triclinic form. An additional closer inspection demonstrated that some phases were very similar to each other: in those cases the ones with lower symmetry were, in fact, slightly distorted cells of those with higher symmetry, with differences of around 1% in their

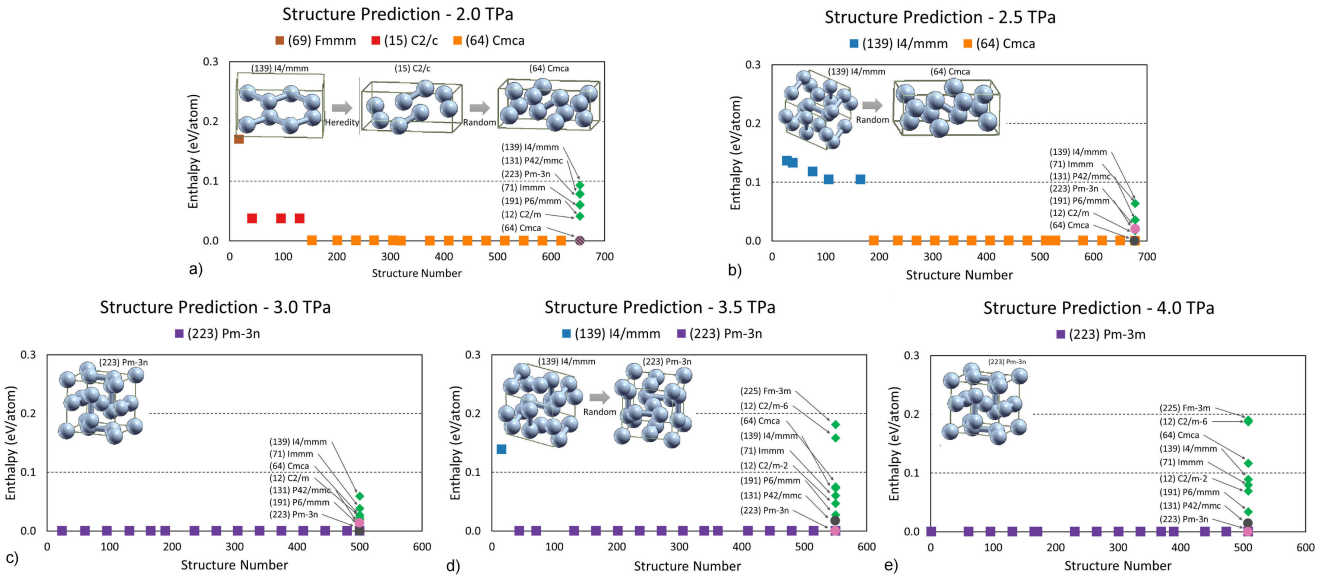

FIGURE 2. Structure prediction process for fluorine with 8 atoms per cell within the pressure range from 2.0 to 4.0 TPa. The squares show the lowest enthalpy obtained at a given generation, with the colors indicating the space group of the best individuals: $C2/c$ (red), $Fmmm$ (brown), $Cmca$ (orange), $I4/mmm$ (blue), and $Pm\bar{3}n$ (purple). The insets show as 3D-images the sequences in the process of predicting the best structures by using the genetic algorithm implemented in USPEX. Relative enthalpies from Ref. [13, 15] are in gray and pink circles, respectively.

TABLE II. K-point grids for the final phases of high-pressure fluorine.

Phase	k-point grid
(12) $C2/m-2$	$16\times16\times12$
(71) $Immm-2$	$16\times16\times12$
(139) $I_4/mmm-2$	$12\times16\times16$
(225) $Fm\bar{3}m-4$	$12\times12\times12$
(12) $C2/m-6$	$12\times16\times12$
(15) $C2/c-8$	$4\times4\times4$
(64) $Cmca-8$	$16\times16\times16$
(131) P_{42}/mmc	$16\times16\times16$
(223) $Pm\bar{3}n$	$16\times16\times16$

cell parameters and atomic positions. This realization allowed us to narrow the list down to 9 structures: $C2/m-2$, $Immm$, I_4/mmm, $Fm\bar{3}m$, $C2/m-6$, $C2/c$, $Cmca$, P_42/mmc, and $Pm\bar{3}n$. More detailed calculations were carried out for the final set of structures. For instance, additional physical properties were calculated using Quantum ESPRESSO with a projector-augmented wave pseudopotential including seven valence electrons. For all final calculations, the kinetic energy cutoff for the plane-wave basis set was 200 Ry and their correspondent k-point grid for the Brillouin zone integration provided a total energy difference convergence of 2 meV per atom or better. The details are displayed in Table II.

Figure 2 shows the case of 8 atoms per cell at selected pressures after variable-cell optimization from *ab initio* results for the forces and cell stresses. USPEX was able to predict those phases proposed in previous works [13, 15] after just a few iterations. The insets show structures with the best individual enthalpy per atom at each generation; the squares mark the minimum enthalpy corresponding to different space groups:$C2/c$ (red), $Fmmm$ (brown), $Cmca$ (orange), $I4/mmm$ (blue), and $Pm\bar{3}n$ (purple). Each green rhombus indicates the relative enthalpy of other structures obtained with USPEX and those reported in Refs. [13, 15] are in gray and pink circles, respectively.

Figure 3, the enthalpy relations for the structures found in this work, along with those previously proposed, are represented. The molecular phase $Cmca$ remains stable up to

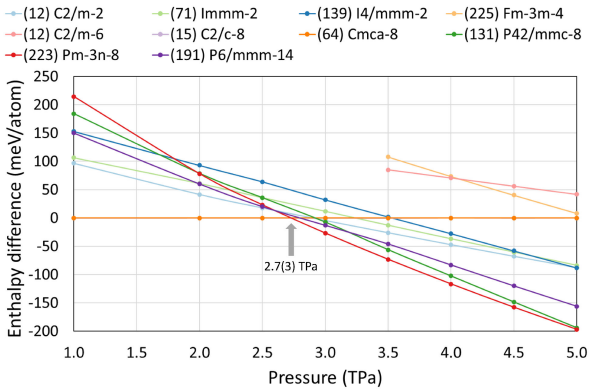

FIGURE 3. Enthalpy relations of the structures found with the USPEX code and those reported in Refs. [13,15], relative to the $Cmca$ structure as a function of pressure. The final number after the dash, in the name of each structure, represents the number of atoms per conventional unit cell.

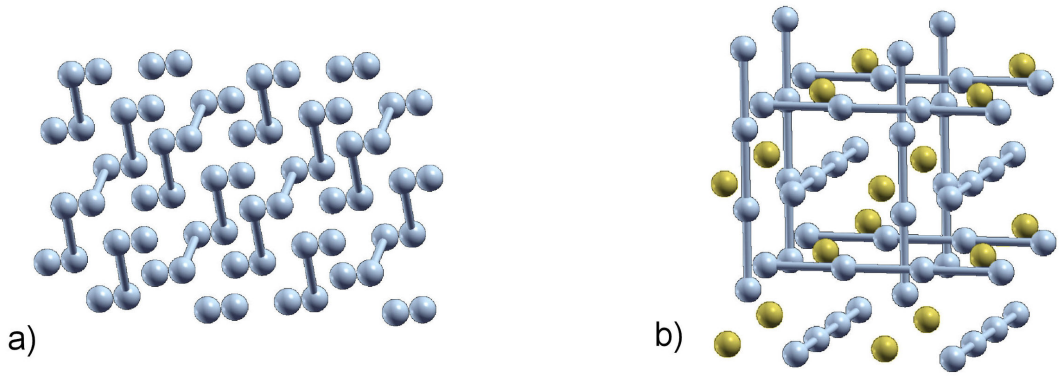

FIGURE 4. Fluorine primitive cell of a) molecular $Cmca$ at 1.0 TPa, and b) polymeric-atomic $Pm\bar{3}n$ at 4.0 TPa consisting of linear chains (gray spheres) and atoms residing in the voids between chains (yellow).

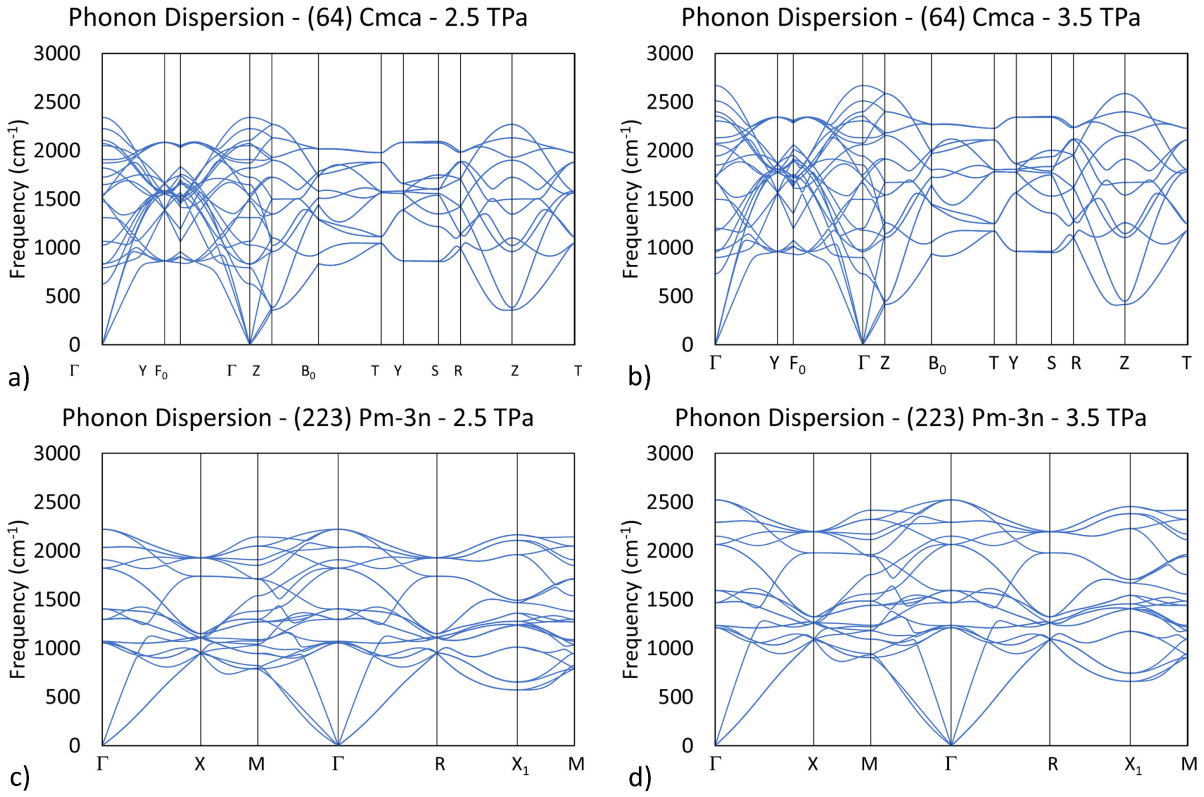

FIGURE 5. Phonon dispersion relations of $Cmca$ at a) 2.5 TPa and b) 3.5 TPa, and $Pm\bar{3}n$ c) 2.5 TPa and d) 3.5 TPa.

2.7(3) TPa. This persistence of the phase $Cmca$ up to the terapascal regime was also reported in Ref. [15], and our USPEX calculations confirm that statement. $Cmca$ transforms directly into $Pm\bar{3}n$, which was also reported as a stable form for solid fluorine by Olson *et al.* [13] and Duan *et al.* [15]. Nevertheless, in those two previous references the $Pm\bar{3}m$ phase emerges at a higher pressure and after a reported intermediate phase: $P4_2/mmc$ for Ref. [13] and $P6/mmc$ for Ref. [15], which represent contradictory findings. In fact, our USPEX results found the phase $P4_2/mmc$ (green line in Fig. 3) which shows an interesting tendency, but its enthalpy is not the lowest at any pressure within the range of our current study, although the situation could change at higher pressures. On the other hand, since the $P6/mmc$ structure reported in Ref. [15] did not appear in the USPEX search because it has 14 atoms per cell, we included it manually in our calculations and its enthalpy is also plotted (violet line in Fig. 3). However, same as for $P4_2/mmc$, $P6/mmc$ also does not become the most stable within our pressure range, therefore, our results do not support the findings from previous works regarding the existence of an intermediate phase between $Cmca$ and $Pm\bar{3}n$ at zero temperature.

Regarding the two most stable structures found in this work, we can conclude that $Cmca$ is a molecular phase, since, for example at 1.0 TPa, the nearest F–F distance is calculated as 1.28 Å, and the second nearest F–F distance is

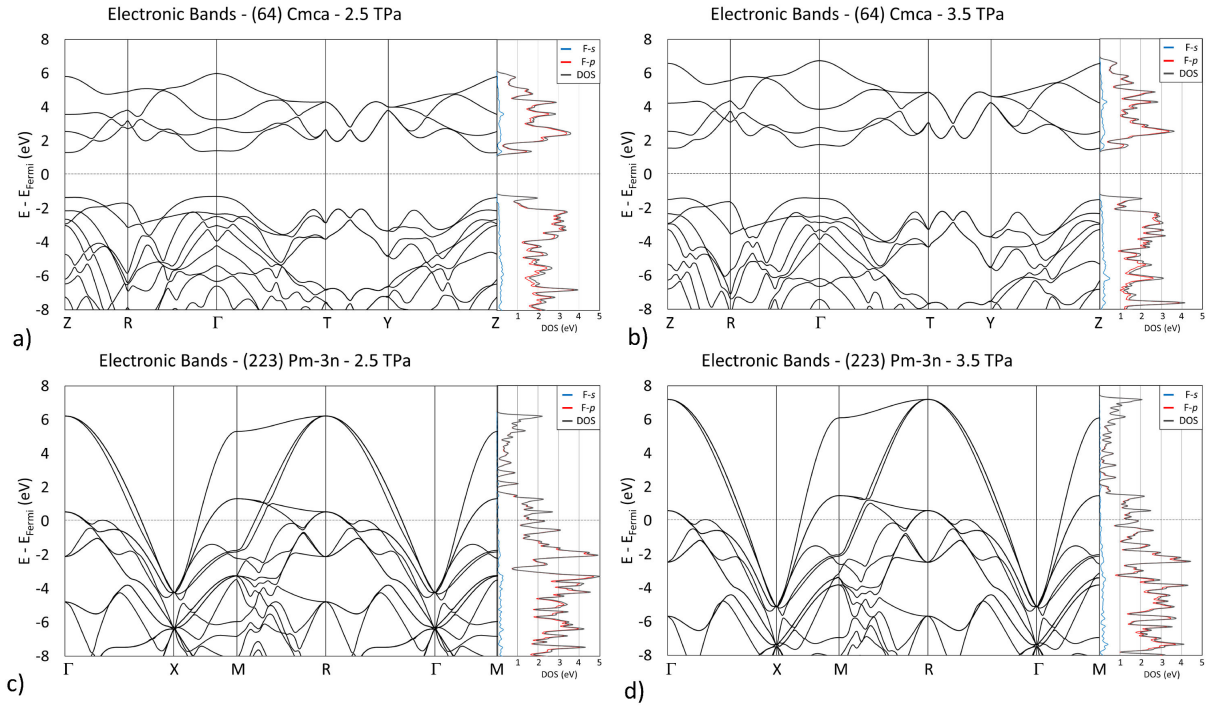

FIGURE 6. Band structure and partial density of states (PDOS) of $Cmca$ at (a) 2.5 TPa and (b) 3.5 TPa, and $Pm\bar{3}n$ (c) 2.5 TPa and (d) 3.5 TPa. The orbital s and orbital p contributions, and the total DOS are represented in blue, red, and gray lines, respectively.

1.55 Å, which clearly establishes the molecular character of this crystalline structure which is shown in Fig. 4a). On the other hand, the phase $Pm\bar{3}n$ is composed of two types of F atoms as shown in Fig. 4b): 75% of them (in gray) are polymer linear (1D) chains that go along the lattice vectors, and the remaining 25% (in yellow) are atoms located in the otherwise empty space between the linear chains, as shown in Fig. 4b). The mixed polymeric-atomic F character in phase $Pm\bar{3}n$ is consistent with the reports from Refs. [13, 15]. At 4.0 TPa, the distance between atoms within the polymeric chain is 1.26Å, and the closest distance between an atom located in an interstice and an atom in a linear chain is 1.40Å.

The dynamical stability of structures $Cmca$ and $Pm\bar{3}n$ has been established through phonon calculations which demonstrate that they are stable as a function of pressure across the phase transition, as represented in Fig. 5. From a mechanical perspective, an observed increase in frequencies with increasing pressure shows that the phonon modes of phases $Cmca$ and $Pm\bar{3}n$ become stiffer, hinting to a more rigid structure. This observation is significant as it suggests that these structures are able to withstand increased stress and deformation without undergoing structural deformation or collapse.

In addition to the phonon calculations, electronic band structures were also computed on both systems. At pressures below and above the transition, phase $Pm\bar{3}n$ was found to be a metal according to an absence of gap at the Fermi level in its electronic band structure [Figs. 6c) and d)]. On the other hand, $Cmca$ is a wide-gap semiconductor and our calculations revealed that at 2.5 TPa [Fig. 6a)] it has a band-gap of

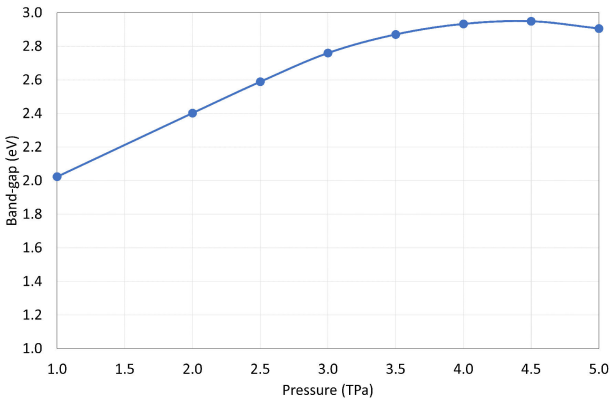

FIGURE 7. Variation of band-gaps for $Cmca$ as a function of pressure.

2.6 eV which increases to 2.9 eV at 3.5 TPa [Fig. 6b)]. The behavior or this band-gap as a function of pressure is shown in Fig. 7 for the pressure range spanned in this study, showing an unusual behavior below 4.5 TPa, since, for most materials, applying pressure is a well known way to induce metallization, still, fluorine is not alone in this exotic behavior [26] where the ability to lower the energy by forming insulating closed-shell electronic structures wins over the tendency to lower the energy of the system by delocalizing the electrons. Finally, as expected, it is observed that the contributions to the total electronic density of states (DOS) for the two main phases in this study come primarily from the orbital *p*, rather than orbital *s*, however, while for the case of $Pm\bar{3}n$ the projection on the orbital *s* is basically non-existing at energies that are close or above the Fermi energy, the contribution of

that same orbital appears clearly also above the Fermi level for the case of $Cmca$, pointing to a sp-type of hybridization in that molecular phase.

4. Conclusions

In summary, the evolutionary structural search approach implemented in the USPEX code, supported by DFT for calculating forces and stresses, has been tested at pressure conditions spanning several TPa. We corroborated the existence of a transition from the widely stable $Cmca$ molecular form of fluorine towards a non-molecular phase that is composed of a mixture of linear chains and isolated atoms. So far, the stability of a pure element's molecular solid is one of the highest in fluorine, rivaled only by oxygen that also shares with fluorine its high electronegativity, confirming the heuristic expectation that these two elements should behave similarly in many ways, among which, being reluctant to become fully polymeric. In fact, an increase in phonon frequencies for $Cmca$ shows that its molecular structure seems to get hardened and more dynamically stable upon compression, at least up to 4.5 TPa when a decrease in its electronic band-gap starts appearing. Previous contradictory reports of intermediate stable phases existing in the transition between $Cmca$ and $Pm\bar{3}n$ were not supported here at zero temperature and, even if it is fair to admit that the energy differences between competing candidates are too small, our results for the stable phases are well converged and do no suffer from numerical errors since within this level of theory they are consistent across many iterations of the structural search process and also at every pressure that was tested in this study. Although beyond of the scope of this work, the phase changes reported here at high pressure may be the initial step towards further work on this element, *i.e.*, calculating the finite temperature contributions to the free energy for determining how the relative stability of the different structures may change. Finally, this work may be the inspiration for exploring the behavior of other halogen elements at high pressure.

5. Acknowledgements

B. H. C.-O. thanks the financial support from MinCiencias under grant No. 80740-585-2021. J. A. M. thanks the VicerrectorÃa de Investigaciones of the Universidad de Cartagena, for the support of the Grupo de Modelado Computacional through internal grants. The numerical calculations in this article were performed on the ROSMME High-Performance Computing Resource of the University of Cartagena.

1. W. J. Nellis *et al.*, Phase Transition in Fluid Nitrogen at High Densities and Temperatures, *Physical Review Letters* **53** (1984) 1661.
2. R. Reichlin *et al.*, Optical Studies of Nitrogen to 130 GPa, *Physical Review Letters* **55** (1985) 1464.
3. Y. Fujii *et al.*, Evidence for molecular dissociation in bromine near 80 GPa, *Physical Review Letters* **63** (1989) 536.
4. K. Takemura *et al.*, Observation of Molecular Dissociation of Iodine at High Pressure by X-Ray Diffraction, *Physical Review Letters* **45** (1980) 1881.
5. F. van Bolhuis, P. B. Koster, and T. Migchelsen, Refinement of the crystal structure of iodine at 110 K, *Acta Crystallographica* **23** (1967) 90.
6. D. Duan *et al.*, Ab initio studies of solid bromine under high pressure, *Physical Review B* **76** (2007) 104113.
7. Z. Gamba and E. B. Halac, The ordered and disordered phases of crystalline F2, The Journal of Chemical Physics 87 (1987) 7184.
8. K. Kobashi and M. Klein, Lattice vibrations of solid α-F2, *Molecular Physics* **41** (1980) 679.
9. D. Kirin and R. D. Etters, Calculated static and dynamic properties of solid α-F2, *The Journal of Chemical Physics* **84** (1986) 3439.
10. D. Schiferl *et al.*, Raman spectra and phase diagram of fluorine at pressures up to 6 GPa and temperatures between 10 and 320 K, *The Journal of Chemical Physics* **87** (1987) 3016.
11. M. Pravica *et al.*, Note: Loading method of molecular fluorine using x-ray induced chemistry, *Review of Scientific Instruments* **85** (2014) 086110.
12. Q. Lv *et al.*, Crystal structures and electronic properties of solid fluorine under high pressure, *Chinese Physics B* **26** (2017) 076103.
13. M. A. Olson *et al.*, Prediction of chlorine and fluorine crystal structures at high pressure using symmetry driven structure search with geometric constraints, *The Journal of Chemical Physics* **153** (2020) 094111.
14. R. Domingos, K. M. Shaik, and B. Militzer, Prediction of novel high-pressure H2O-NaCl and carbon oxide compounds with a symmetry-driven structure search algorithm, *Physical Review B* **98** (2018) 174107.
15. D. Duan *et al.*, Multistep Dissociation of Fluorine Molecules under Extreme Compression, *Physical Review Letters* **126** (2021) 225704.
16. C. J. Pickard and R. J. Needs, Ab initio random structure searching, *Journal of Physics: Condensed Matter* **23** (2011) 053201.
17. A. R. Oganov and C. W. Glass, Crystal structure prediction using ab initio evolutionary techniques: Principles and applications, *The Journal of Chemical Physics* **124** (2006) 244704.
18. C. W. Glass, A. R. Oganov, and N. Hansen, USPEX-Evolutionary crystal structure prediction, *Computer Physics Communications* **175** (2006) 713.
19. A. R. Oganov, A. O. Lyakhov, and M. Valle, How Evolutionary Crystal Structure Prediction Works-and Why, *Accounts of Chemical Research* **44** (2011) 227.

20. A. O. Lyakhov *et al*., New developments in evolutionary structure prediction algorithm USPEX, *Computer Physics Communications* **184** (2013) 1172.

21. P. Giannozzi *et al*., QUANTUM ESPRESSO: A modular and open-source software project for quantum simulations of materials, *Journal of Physics: Condensed Matter* **21** (2009) 21832390.

22. P. Giannozzi *et al*., Advanced capabilities for materials modelling with Quantum ESPRESSO, *Journal of Physics: Condensed Matter* **29** (2017) 465901.

23. J. D. Pack and H. J. Monkhorst, Special points for Brillouin-zone integrations, *Physical Review B* **16** (1977) 1748.

24. P. E. Blöchl, Projector augmented-wave method, *Physical Review B* **50** (1994) 17953.

25. J. P. Perdew, K. Burke, and M. Ernzerhof, Generalized Gradient Approximation Made Simple, *Physical Review Letters* **77** (1996) 3865.

26. Y. Ma *et al*., Transparent dense sodium, *Nature* **458** (2009) 182.

27. B. H. Cogollo-Olivo *et al*., Phase diagram of oxygen at extreme pressure and temperature conditions: An ab initio study, *Physical Review B* **98** (2018) 094103.